ACS APPLIED MATERIALS & INTERFACES

Research Article

Cite This: ACS Appl. Mater. Interfaces 2017, 9, 37238-37245

www.acsami.org

Clustering of Cyclodextrin-Functionalized Microbeads by an Amphiphilic Biopolymer: Real-Time Observation of Structures Resembling Blood Clots

Chandamany Arya, Camila A. Saez Cabesas, Hubert Huang, and Srinivasa R. Raghavan*

Department of Chemical & Biomolecular Engineering, University of Maryland, College Park, Maryland 20742, United States

Supporting Information

ABSTRACT: Colloidal particles can be induced to cluster by adding polymers in a process called bridging flocculation. For bridging to occur, the polymer must bind strongly to the surfaces of adjacent particles, such as via electrostatic interactions. Here, we introduce a new system where bridging occurs due to specific interactions between the side chains of an amphiphilic polymer and supramolecules on the particle surface. The polymer is a hydrophobically modified chitosan (hmC) while the particles are uniform polymeric microbeads (~160 μm in diameter) made by a microfluidic technique and functionalized on their surface by α-cyclodextrins (CDs). The CDs have hydrophobic binding pockets that can capture the *n*-alkyl hydrophobes present along the hmC chains. Clustering of CD-coated microbeads in water by hmC is visualized in real time using optical microscopy. Interestingly, the clustering follows two distinct stages: first, the microbeads are bridged into clusters by hmC chains, which occurs by the interaction of individual chains with the CDs on adjacent particles. Thereafter, additional hmC from the solution adsorbs onto the surfaces of the microbeads and an hmC "mesh" grows around the clusters. This growing nanostructured mesh can trap surrounding microsized objects and sequester them within the overall cluster. Such clustering is reminiscent of blood clotting where blood platelets initially cluster at a wound site, whereupon they induce growth of a protein (fibrin) mesh around the clusters, which entraps other passive cells. Clustering does not occur with the native chitosan (lacking hydrophobes) or with the bare particles (lacking CDs); these results confirm that the clustering is indeed due to hydrophobic interactions between the hmC and the CDs. Microbead clustering via amphiphilic biopolymers could be applicable in embolization, which is a surgical technique used to block blood flow to a particular area of the body, or in agglutination assays.

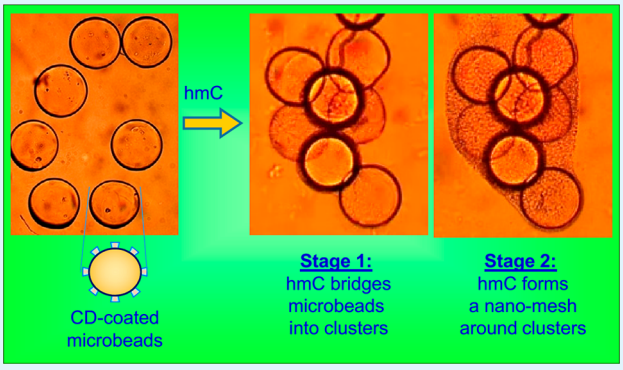

KEYWORDS: *chitosan, associating polymer, hydrophobic interactions, self-assembly, biomimetic materials, microfluidic synthesis*

INTRODUCTION

The interactions between polymers and colloidal particles have been studied for decades and are well-described in standard textbooks.[1,2] It is known that polymers can induce the clustering (also termed aggregation, flocculation, or agglutination) of particles by two main mechanisms: bridging or depletion flocculation.[1−3] While the latter deals with polymers that do not adsorb or bind to the particles, bridging flocculation requires a strong affinity between the polymer chains and the particles.[3,4] That is, one segment of a long polymer chain binds to one particle while another segment of the same chain binds to an adjacent particle; in effect, the chains *bridge* the particles into clusters. Bridging flocculation has been studied extensively by both experiments[4−6] and simulations,[7,8] and it also has practical applications, such as in the removal of suspended matter during wastewater treatment.[3,9] Typically, the affinity between the particles and polymer chains is tuned via electrostatic interactions; that is, if the particles have a negative surface charge, then a positively charged polymer is used to induce bridging flocculation.[4−6]

More recently, researchers have investigated other modes for inducing particles to cluster due to polymer bridging. To make the clustering highly specific, biomolecular interactions have been invoked.[10−14] In one scenario, strands of DNA were introduced on the surfaces of the particles.[12] To induce clustering, long DNA chains with complementary sequences were introduced into the solution. The added DNA formed base pairs with the DNA strands on adjacent particles and thereby bridged the particles into clusters. Specific clustering has also been induced by protein−ligand or antibody−antigen interactions.[10] Since proteins and antibodies are often very compact, polymer tethers may need to be used for bridging. In one example, two types of particles (A and B) were used, both

Received: April 18, 2017
Accepted: September 25, 2017
Published: October 10, 2017

DOI: 10.1021/acsami.7b05435
ACS Appl. Mater. Interfaces 2017, 9, 37238−37245

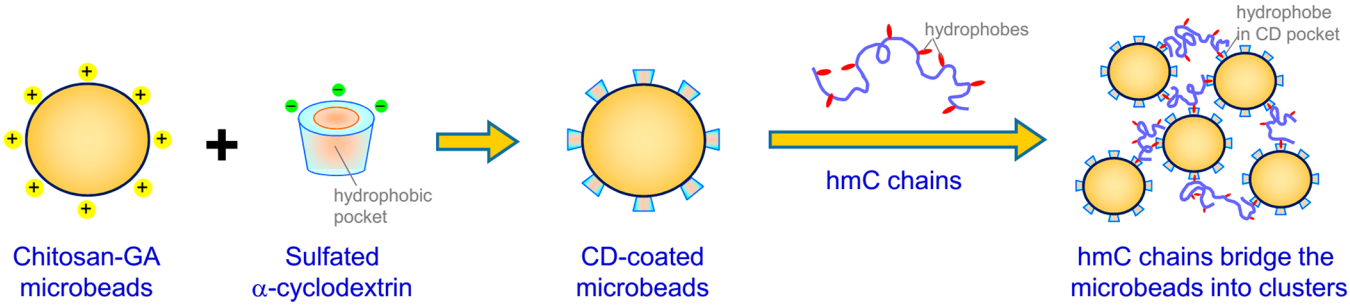

Figure 1. Schematic representation of this study. Microbeads formed by cross-linking the biopolymer chitosan with glutaraldehyde (GA) have a cationic surface. These are functionalized with CDs by incubation with sulfated α-CD. The resulting CD-coated microbeads are combined with hydrophobically modified chitosan (hmC), which is shown with a hydrophilic backbone in blue and hydrophobic tails in red. The hmC sticks its hydrophobes into the binding pockets on the CDs, and thereby the microbeads are bridged into clusters.

having long polymeric tethers.[10] The tether to A was functionalized with a protein while the tether to B was functionalized with the ligand to the above protein. Upon combining the A and B particles, heteroclusters containing both particle types were formed due to the binding of proteins with their ligands.

In this study, we present a new mode for bridging specific microparticles into clusters by a specific kind of polymer. The driving force in our case is the affinity between hydrophobic chains on the polymer and supramolecules (with hydrophobic binding pockets) anchored onto the particle surface. We were inspired to create this system following earlier work from our lab on amphiphilic biopolymers such as hydrophobically modified chitosan (hmC).[15−18] In particular, hmC (with n-alkyl hydrophobic tails, n = 12−18) transforms suspensions of vesicles,[15,17] blood cells,[16,18] and other mammalian cells[18] into self-supporting gels. Such gelation was shown to be due to polymer bridging, where the hmC chains stick their hydrophobic side chains into the hydrophobic bilayers of vesicles or cells and thereby form sample-spanning clusters.[15−18] Moreover, we showed that the addition of α-cyclodextrin (CD), a sugar-based supramolecule, reverses the gelation by hmC.[16−18] This is because the CDs have binding pockets that have a strong affinity for the single-tailed hydrophobes on hmC.[19,20]

From the above findings, we hypothesized that particles with CDs on their surface would also be able to bind hmC chains. This study began in an attempt to test the hypothesis. We create polymeric microbeads by a microfluidic approach[21] and functionalize their surfaces with CDs. When these CD-coated microbeads are combined with an hmC having n-C_{12} tails, a two-stage clustering process occurs, which is visualized in real time using optical microscopy. It is shown that this clustering process is reminiscent of blood clotting.[22,23] Our study thus should be of interest to both the soft-matter and biomedical communities. Indeed, polymer-induced clustering could also have biomedical utility. One possibility is in the surgical technique of embolization, where an embolus (typically a cluster of microscale or millimeter-scale gel particles) is placed in particular blood vessels.[24−26] The purpose of embolization is to block the flow of blood to a particular area of the body, for example, to starve a tumor of its blood supply, to prevent internal hemorrhaging, or to curtail an aneurysm. Clustering or agglutination of microparticles can also serve as the basis for biological assays, including for the detection of pathogens.[13,14,27]

■ MATERIALS AND METHODS

Materials and Chemicals. The following chemicals were obtained from Sigma-Aldrich: the biopolymer chitosan (molecular weight of 190000−310000, degree of deacetylation ∼80%), the nonionic detergent Span 80, glutaraldehyde (GA) (grade 1, 70%), the solvents ethanol, hexadecane, and 1-decanol, sodium chloride (NaCl), α-cyclodextrin sulfated sodium salt hydrate (CD-sulfate), and fluorescein-5-EX N-hydroxysuccinimide ester (NHS-fluorescein). Red-fluorescent latex nanospheres (nominal diameter of 100 nm, with surface carboxylate groups) were purchased from Life Technologies (Cat #F-8801). Carbon black particles (N110) were obtained from Sid Richardson Carbon Company and iron oxide (γ-Fe_2O_3) nanoparticles (with a surface area ∼42 $m^2\ g^{-1}$) were purchased from Alfa Aesar.

Synthesis of Microbeads. Microbeads of chitosan-GA were prepared in the same manner as described in our earlier paper.[21] A coflow microfluidic device was constructed by inserting a silica capillary (150 μm i.d., from SGE Analytical Science) into commercial Teflon tubing (300 μm i.d., from Cole Parmer). A schematic and a photograph of this device are shown in Figure S1 of the Supporting Information. An aqueous solution of 2 wt % chitosan in 0.2 M acetic acid was fed through the inner capillary at 1.5 μL/min. The oil phase (hexadecane with 2 wt % Span 80) was sent through the outer tube at 30 μL/min. In the process, uniform aqueous droplets with a diameter of ∼160 μm were formed, and these were collected in a cross-linking solution of 2 wt % GA in hexadecane (with 2 wt % added Span 80). The droplets were allowed to cross-link for 20 h to form the chitosan-GA microbeads. These were then washed three times each with ethanol and deionized (DI) water, and ultimately stored in DI water. For the microbeads containing carbon black, the chitosan solution was first mixed with 1 wt % carbon black before being fed through the device. Similarly, for the magnetic microbeads, 0.5 wt % of the γ-Fe_2O_3 nanoparticles was dispersed in the chitosan solution before it was passed through the device.

Functionalization of Microbeads. To a suspension of chitosan-GA microbeads (1000 beads/mL) in acetic acid (pH of 4.5), sulfated α-cyclodextrin (5 wt %) was added and allowed to react for an hour under gentle mixing. The CD concentration used here was in large excess of that needed for saturating the surface of the beads. The CDs attached to the microbead surface through electrostatic interactions. Thereafter, the microbeads were washed five times with acidic water (pH 4.5) and were stored as a suspension in acidic water prior to use in the clustering experiments.

Synthesis of Functionalized Polymers. The hmC used here had C_{12} hydrophobes and was synthesized by reacting the parent chitosan with n-dodecyl aldehyde, as described in the literature[28] and in our earlier studies.[15,16] The degree of hydrophobic substitution follows the reaction stoichiometry[15] and here it was fixed at 5 mol % of the available amine groups on the parent chitosan. Fluorescently labeled hmC was prepared by reacting the polymer with NHS-fluorescein, following procedures described in the literature.[29]

DOI: 10.1021/acsami.7b05435
ACS Appl. Mater. Interfaces 2017, 9, 37238−37245

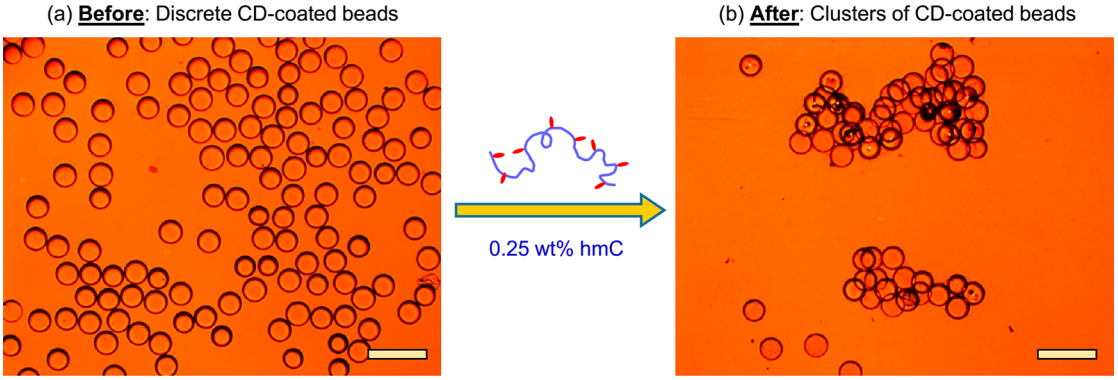

Figure 2. Clustering of CD-coated microbeads by hmC. Optical micrographs are shown of (a) the initial CD-coated microbeads, which are discrete and not in clusters, and (b) the same after adding 0.25 wt % hmC, where most of the initial microbeads are in large clusters induced by the bridging of hmC chains. Scale bars are 600 μm.

Studies on Polymer-Induced Clustering of Microbeads. For these studies, the hmC was dissolved in aqueous salt solution (0.9 wt % NaCl). From a stock solution of CD-coated chitosan-GA beads in acidic water (1000 beads/mL), 25 μL was taken and added to a glass slide mounted on an inverted microscope. Then 25 μL of the hmC solution at a given concentration was added. A micropipette tip was used to gently mix the sample for a few seconds.

Optical and Fluorescence Microscopy. A Zeiss Axiovert 135 TV inverted light microscope equipped with ToupView Imaging software was used for bright-field microscopy. Images were obtained with either a 2.5× or 10× objective. To observe fluorescence from the nanospheres, images were taken using a band-pass excitation filter (530−585 nm) and a long-pass emission filter at 615 nm. In the case of the fluorescent hmC, an excitation filter at 480 nm and an emission filter at 510 nm were used.

RESULTS AND DISCUSSION

The components of our system are shown in Figure 1. We start with microbeads produced in-house by coflow microfluidics using capillary tubing.[21] Aqueous droplets bearing the biopolymer chitosan are introduced into a reservoir of glutaraldehyde (GA), whereupon the droplets become uniformly cross-linked into near-monodisperse beads (diameter ∼160 μm). Since chitosan is cationic, the beads are expected to retain significant residual positive charge on their surface. To confirm this, we first exposed the chitosan-GA microbeads to 100 nm anionic (carboxylate-functionalized) nanoparticles (NPs) labeled with a red fluorescent dye. After exposure for 30 min, the beads were washed extensively and then examined in a fluorescence microscope (Figure S2). We found substantially higher (2.5×) fluorescence for the NP-coated beads (Figure S2b) relative to the bare beads (Figure S2a). (Note that the latter shows a weak autofluorescence,[30] which is why the signal is nonzero in their case.) This result demonstrated the binding of anionic NPs to the cationic bead surface; clearly, the binding was strong enough that the NPs were not removed by extensive washing. Also, the binding of NPs to the beads was much lower if the two were incubated in the presence of salt (2 M NaCl), as shown by Figure S2c. Salt is known to screen and thereby diminish the electrostatic attractions between charged species.[1,2] Thus, the results from Figure S2 confirm that electrostatic interactions can be used to bind anionic species to the surfaces of chitosan-GA beads.

On the basis of the above results, we proceeded to functionalize chitosan-GA microbeads with CDs. An anionic form of α-CD, that is, sulfated α-CD (Figure 1), was combined with the beads for a period of 1 h. After this step, the beads were washed extensively and stored in aqueous solution, where they remained stable without aggregation. At this stage, we expect the bead surface to be coated to saturation by CDs (Figure 1). This CD coating remains persistent and stable with time, at least over a period of a week. That is, both freshly prepared beads as well as beads stored for a week gave identical results in the experiments described below.

We proceeded to study the effect of adding hmC to the CD-coated beads, as indicated by Figure 1. The experiments were done under an optical microscope to allow changes to be observed in real time. At t = 0, the beads are discrete and unaggregated (Figure 2a), and at this point, the hmC is added. We use a micropipette tip to gently mix the sample on the microscope slide for a few seconds. Thereafter, almost instantly, large clusters of the beads are formed (Figure 2b). The clusters are essentially irreversible and remain unchanged for subsequent time. Note from Figure 2b that almost all the initial beads are incorporated into the clusters. That is, at the hmC concentration used in this experiment (0.25 wt % hmC in the final sample), the fraction of beads that are in clusters is >80%. We also conducted the same experiment at lower hmC concentrations. The results are shown in Figure 3 as a plot of the percentage of beads that are clustered versus hmC concentration. The plot shows that the extent of clustering increases with hmC concentration and ultimately saturates at a value >80%. These data are akin to an adsorption isotherm; however, the data at low hmC concentrations (<0.1 wt %) are

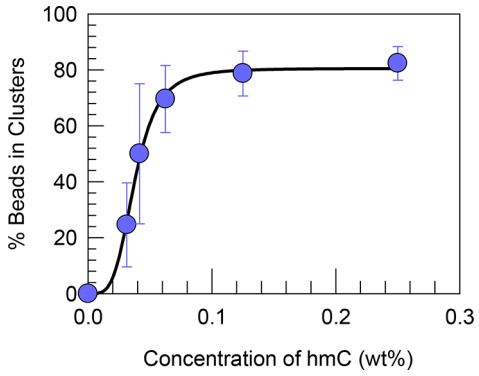

Figure 3. Effect of hmC concentration on the extent of clustering. The fraction of microbeads in clusters for each hmC concentration is plotted. Error bars represent the standard deviations across multiple experiments. The line through the data is to guide the eye.

DOI: 10.1021/acsami.7b05435
ACS Appl. Mater. Interfaces 2017, 9, 37238−37245

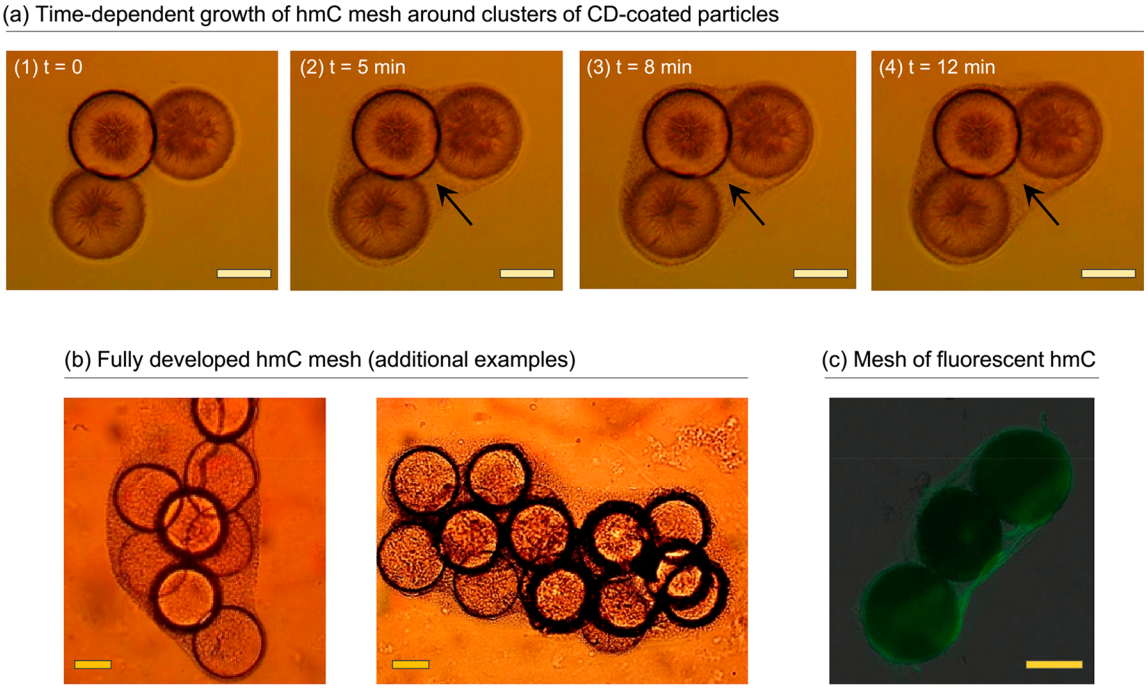

Figure 4. Second stage of the clustering process, where a mesh of hmC grows around the initial clusters of CD-coated microbeads. (a) Time-dependent growth of the hmC mesh around a cluster of three CD-coated microbeads. These are still images taken from Movie 1 (Supporting Information). The mesh, indicated by arrows in images 2−4, is fully developed by about 12 min after addition of hmC to the microbeads. (b) Optical micrographs of two other instances where a fully developed hmC mesh surrounds large clusters of CD-coated microbeads. (c) Fluorescence micrograph of the hmC mesh around a cluster of CD-coated microbeads. In this case, the hmC was functionalized with fluorescein, and the green color indicates that the mesh is composed of hmC. Scale bars are 100 μm in all images.

quite noisy, and this precludes us from elucidating the precise form for the underlying relationship over the entire concentration range. Nevertheless, the results are very consistent and repeatable at 0.25 wt % hmC and above. Therefore, we fixed the concentration at 0.25 wt % hmC in subsequent experiments.

Figure 2 shows that clustering is induced upon adding hmC to CD-coated beads. To confirm the specific nature of this clustering, we performed a series of control experiments. First, we incubated the CD-coated beads with native (unmodified) chitosan. No clustering was observed at the polymer concentrations tested. Representative images are shown in the top panel of Figure S3. Next, we studied the bare microbeads that did not have CDs on their surfaces. These did not cluster when exposed to hmC at the concentrations tested. An additional control was done by taking the bare beads and first exposing them to sodium sulfate (Na_2SO_4) salt as a surrogate for the sulfated CD. The beads were then washed and exposed to hmC; again, these did not cluster. Taken together, these observations allow us to rule out alternate causes for clustering such as electrostatic or other nonspecific binding of polymers to bead surfaces. We conclude that clustering is indeed caused by specific interactions between the *hydrophobes* on hmC chains and the *hydrophobic binding pockets* of the CDs on the beads, as shown by Figure 1. In turn, such hydrophobic interactions result in bridging flocculation of the beads by hmC chains.

It is useful to compare the structure of the clusters in Figure 2 with those observed in previous studies of bridging flocculation,[4−6] especially via simulations.[7,8] Dickinson and Euston[7] found through their Monte Carlo simulations that clusters became larger and more compact as the strength of the attractive interactions between the polymer and the particles increased. When the attractions were weak, the clusters were loose, with some particles bridged by long, dangling chains. However, when the attractions were strong, the clusters were compact, with very short distances between any two particles within a cluster. The bridges then served as a "polymeric glue" between adjacent particles, and most of the particles were incorporated within clusters (i.e., there were hardly any unaggregated particles). These results are broadly consistent with the structure of our clusters in Figure 2. We can therefore infer that our system is one in which bridging occurs due to strong attractive interactions (between the hmC and the CDs); these interactions are evidently much stronger compared to the nonspecific electrostatic interactions that typically drive bridging flocculation.

Further interesting changes are observed in the hmC + CD-coated bead system as time progresses (Figure 4a). As mentioned, the initial clustering of beads occurs rapidly (within 1 min of contacting the beads with hmC; image 1). Subsequently, we observe the growth of a precipitate around the clusters over the course of the next 10−15 min. A movie of this process is provided as Movie 1 in the Supporting Information, and still images from this movie are shown in images 1−4. The precipitate, indicated by arrows in the images, appears to be a porous mesh and it coats all the beads in the cluster. Note that there is no such mesh in the surrounding bulk solution. The mesh forms around all CD-coated beads, including single beads that are not in clusters. Also, the mesh forms around clusters of all sizes, and two examples of large clusters covered with a mesh are shown in Figure 4b. We believe this nanostructured mesh is generated by multilayer adsorption of hmC chains onto the surfaces of CD-covered beads, and it is evidently due to the strong binding interactions

DOI: 10.1021/acsami.7b05435
ACS Appl. Mater. Interfaces 2017, 9, 37238−37245

between the two. We further verified the identity of the mesh by labeling hmC with a green fluorescent dye and combining it with CD-coated beads. The mesh in Figure 4c around the cluster shows a green fluorescence, indicating that it is indeed composed of hmC chains.

Additional experiments provide insight into the hmC mesh formation. First, we combined a solution of hmC (0.1 wt %) in a vial with sulfated α-CD (5 wt %). In this case, a precipitate forms in solution (Figure 5). The precipitate is a low-density layer that fills the top half of the vial, hence, our use of the term "mesh" to describe it. Note that such a mesh does not form if the hmC is combined with neutral α-CD, that is, with CD lacking the sulfate groups. Thus, we conclude that the mesh in the case of hmC + sulfated α-CD arises due to a combination of hydrophobic and electrostatic interctions between the two. We also considered the scenario where bare microbeads (i.e., without a surface coating of CDs) are combined with both the sulfated α-CD and the hmC. In this case (Figure S3, bottom panel), the beads remain unclustered and a precipitate forms in the solution around the beads (there is no affinity between the precipitate and the beads). Thus, it is only when we have beads precoated with CDs that the hmC mesh nucleates and grows around the bead clusters. On the whole, the mesh appears to be akin to a dense aqueous network of hmC chains. We expect that the mesh will have a finite yield stress, but it is not a free-standing solid.

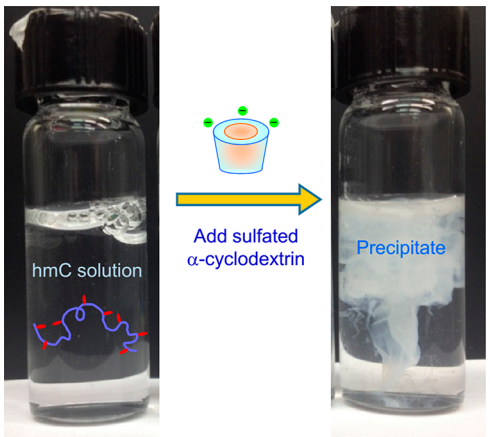

Figure 5. Effect of adding sulfated α-CD to an hmC solution. To a vial containing 0.1 wt % hmC solution, 5 wt % of sulfated α-CD is added. A low-density whitish layer (precipitate) is formed in the vial.

From the above experiments, it is clear that CD-coated beads have a very different interaction with hmC compared to uncoated ("inert") beads. To explore this difference further, we prepared two populations of beads and studied their mixtures. One set of beads was identical to those above: they had a diameter of 160 μm, were transparent, and were coated with CDs. The other set of beads were slightly smaller, with a diameter of 125 μm. Moreover, to distinguish these beads easily, we encapsulated carbon black (CB) nanoparticles in their core (this was done by including 1 wt % CB in the polymer solution used as the dispersed phase in our microfluidic setup).[21] The CB-containing beads were black and opaque, and they were also inert; that is, there were no

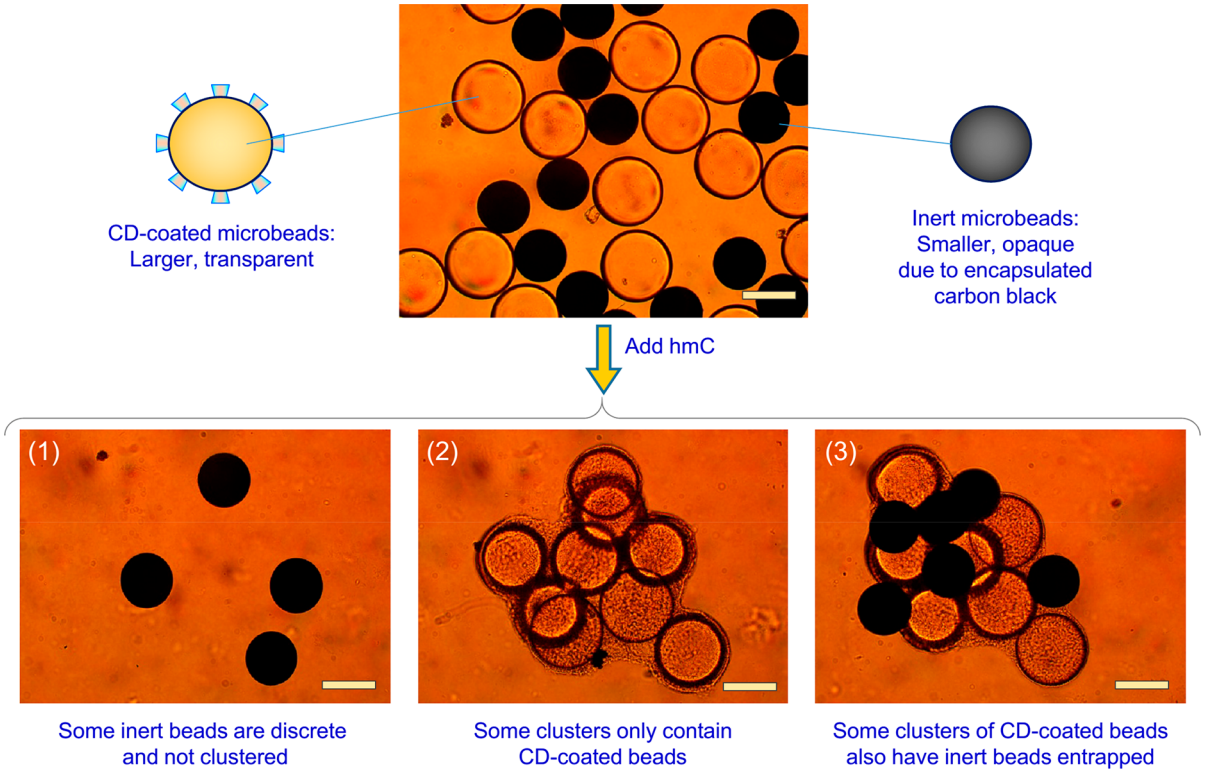

Figure 6. Clustering induced by hmC in a mixture of CD-coated and inert microbeads. The CD-coated microbeads are transparent and have a diameter of 160 μm. The inert microbeads are smaller (diameter of 125 μm) and are opaque due to encapsulated carbon black. Initially (top), there are approximately an equal number of the two, and all the microbeads are unaggregated. Upon adding hmC, different structures are observed, as indicated by images 1−3. Image 1 shows some inert microbeads that are not in clusters. Image 2 shows a large cluster containing only CD-coated microbeads. Image 3 shows a large cluster of CD-coated microbeads in which several inert microbeads are entrapped. Scale bars are 125 μm.

DOI: 10.1021/acsami.7b05435
ACS Appl. Mater. Interfaces 2017, 9, 37238−37245

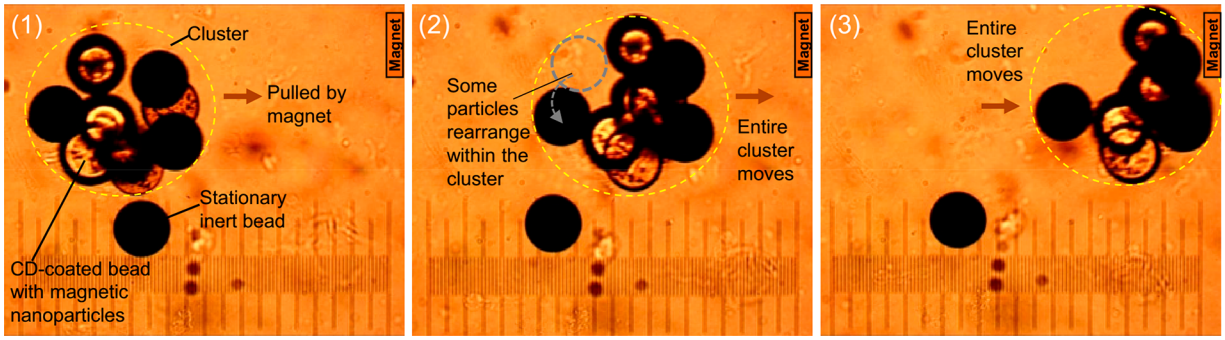

Figure 7. Magnetic transport of a whole cluster. The CD-coated microbeads are transparent and have MNPs in them, while the black beads are inert (no CD coating or MNPs). Images 1−3 are stills at 3 s intervals from Movie 2 (Supporting Information). Initially, in image 1, a number of inert microbeads are trapped in a cluster of the CD-coated microbeads, due to the sticky hmC mesh. When a magnet is introduced to the right of this cluster, the whole cluster moves toward the magnet (from left to right), and this motion is revealed by images 2 and 3. The outline of the cluster is shown by the dashed yellow circle. A microscope scale (1 mm long) is placed at the bottom of the image to provide a frame of reference. Also, the inert microbead below the cluster remains stationary throughout the experiment. Note that as the cluster moves, there is some rearrangement of the inert microbeads within the cluster, as shown by the dashed gray outline and arrow.

CDs on their surfaces. We combined the CD-coated and inert beads in roughly equal ratios (Figure 6, top) and added 0.25 wt % hmC. The resulting images reveal three distinct cases. Some of the inert beads remain as individual entities (i.e., do not cluster) (image 1) and there is no hmC mesh around these beads. In contrast, the CD-coated beads are mostly clustered, and all these clusters have an hmC mesh around them (images 2 and 3). In some cases, the clusters contain only the CD-coated beads (image 2). In other cases, the clusters also have several inert beads trapped in them (image 3). Evidently, as the hmC mesh grows around the clusters, it is capable of entrapping inert objects that are in the vicinity.

Our observations suggest an analogy between the clustering phenomena seen here and the phenomenon of blood clotting. This analogy is illustrated by the schematics in Figure S4. The purpose of the clotting cascade in our body is to create a clot and thereby plug any breach in the endothelium.[22] The main components in this cascade are the blood platelets (a type of blood cell) and two proteins in blood plasma, viz. fibrinogen and thrombin.[22,23] In the first stage, the platelets aggregate to form "platelet plugs" that act as a temporary barrier at the breach location.[22] The initial clustering of CD-coated beads is similar to the formation of a platelet plug. In the next stage, the protein, fibrinogen, binds to the platelet surfaces through activated receptors. At the same time, thrombin activates the polymerization of soluble fibrinogen into insoluble fibrin.[23] Thick strands of fibrin form a visible mesh around the platelets, and these together constitute the clot. The analogous stage in our case is the growth of an (insoluble) hmC mesh around the CD-coated beads. The fibrin mesh entraps surrounding red blood cells, which are not active participants in the clotting cascade, and this ensures that the wound is plugged, that is, that there is no further blood loss.[22] Similarly, here also, inert beads get trapped in the hmC mesh that forms around the initial cluster of CD-coated beads. Lastly, it is worth pointing out that, much like regular blood clots eventually become degraded by the enzyme plasmin, our "artificial clots" are also expected to be enzymatically degradable. Because both the hmC mesh as well as the CD-coated beads are based on the bioopolymer chitosan, they can be degraded by enzymes called chitosanases.[31,32] Indeed, we have previously shown that chitosanases can degrade both aqueous hmC gels[31] as well as capsules based on chitosan.[32]

The above polymer-induced clustering could be useful in surgical embolization, where an embolus, that is, an artificial clot, is placed in particular blood vessels (so as to block blood flow to a tumor, for example).[24−26] One could envision sending an initial pulse of CD-coated beads into specific blood vessels through a catheter, followed by a pulse of polymer (hmC) solution to induce the beads to cluster. The extent of clustering and the strength of the final "clot" can be tuned by the bead concentration, the hmC concentration, and also by the ratio of CD coated to inert beads. With regard to the latter, this is akin to different ratios of platelets and red blood cells (RBCs). Our microscopy experiments reveal distinct morphologies for the clusters in cases where either the CD-coated or the inert beads are in large excess (Figure S5). When there is an excess of CD-coated beads (Figure S5A), large clusters are formed, and most of the inert beads are trapped in them. In contrast, when the inert beads are in excess (Figure S5B), the clusters formed are smaller and have fewer beads in them. Many of the inert beads are found to be discrete and not included in any cluster.

The trapping of inert objects within an hmC-mesh-covered cluster also suggests a means to extract and transport microscale objects. To demonstrate this, we encapsulated magnetic nanoparticles (MNPs) in the CD-coated (transparent) beads.[21] This was done by including 0.5 wt % MNPs in the polymer solution used as the dispersed phase in our microfluidic setup. The above beads were combined with inert and nonmagnetic beads that are black due to the CB in them; see Figure 7. The inert beads represent hypothetical material that needs to be extracted from the system and moved toward a desired location. When hmC is added, as seen earlier, many of the inert beads are trapped in the hmC mesh generated around the CD-coated beads (image 1). Next, when a bar magnet is placed near the sample at one end, entire clusters are attracted to the magnet due to the MNPs in the beads. We can thereby move whole clusters, together with the inert beads that are trapped in them. Images 1−3 in Figure 7, which are stills from Movie 2 (Supporting Information), show the magnetic transport of a given cluster. In these images, note the uncaptured inert bead below the moving cluster, which remains stationary and thus provides a frame of reference for the movement. Also, note that the beads in the cluster are only loosely trapped; as a result, they undergo some rearrangement within the cluster while the cluster is being moved. Never-

DOI: 10.1021/acsami.7b05435
ACS Appl. Mater. Interfaces 2017, 9, 37238−37245

theless, the hmC mesh is "sticky" and thus ensures that all the beads remain confined within the cluster.

CONCLUSIONS

Colloidal Implications. We have developed a new *specific* mode for bridging flocculation (clustering) of colloidal particles by polymers. The clustering occurs only when particles with a particular surface functionality (i.e., CDs, which are supramolecules having a binding pocket for hydrophobes) are combined with polymers having a corresponding functionality (i.e., hydrophobic *n*-alkyl tails). Specific *recognition events* then occur, where the polymer chains insert their tails into the CDs on adjacent particles, thereby bridging the particles together into a cluster. The specific nature of this phenomenon is shown through various control experiments where clustering does not occur: for example, when the polymer lacks hydrophobes or the particles lack CDs. Analogous clustering phenomena have been reported in earlier studies based on specific biomolecular interactions between particles and polymer chains such as DNA base pairing or protein−ligand binding;[10−14] here, we use a much simpler and widely known recognition mode that is based on hydrophobic interactions. We believe many extensions and variations of our study are possible where hydrophobe−CD interactions form the basis for clustering of different colloidal structures.

Biomedical Implications. The other unique aspect of our study arose from our ability to directly visualize clustering in real time using optical microscopy. We found that clustering by hmC of CD-coated microbeads follows *two distinct stages*: first, the beads are bridged into clusters by hmC chains, and then additional hmC from the solution adsorbs and forms a mesh around the clusters. This polymer mesh is able to entrap "bystanders", that is, inert microbeads, within it. If the beads have magnetic properties, the cluster can be moved as a whole by an external magnet. We drew the analogy between this two-stage process and that of blood clotting. The latter also occurs in two stages: first, blood platelets initially cluster at a wound site and form temporary platelet plugs. Next, soluble fibrinogen is converted into an insoluble fibrin mesh around the platelets to form the overall clot, and this entraps other passive cells. We are not aware of similar two-stage cluster development having been reported in colloidal systems, but it is quite likely that analogous phenomena may occur in other cases as well. By changing the ratio of CD-coated to inert beads, we can realize different morphologies of our clusters. We suggest that the ability to form such "synthetic clots" could be useful in surgical embolization.

ASSOCIATED CONTENT

Supporting Information

The Supporting Information is available free of charge on the ACS Publications website at DOI: 10.1021/acsami.7b05435.

Additional figures on the microfluidic setup, microbead clustering, and control experiments (PDF)

Movie 1 depicts the hmC mesh formation, as discussed in Figure 3 (MPG)

Movie 2 shows the movement of whole clusters by an external magnet, as demonstrated in Figure 7 (MPG)

AUTHOR INFORMATION

Corresponding Author

*E-mail: sraghava@umd.edu.

ORCID

Srinivasa R. Raghavan: 0000-0003-0710-9845

Notes

The authors declare no competing financial interest.

ACKNOWLEDGMENTS

This work was partially supported by grants from NSF (DMR-1508155), NIST (70NANB12H238), and the Maryland Industrial Partnerships (MIPS) program.

REFERENCES

(1) Hiemenz, P. C.; Rajagopalan, R. *Principles of Colloid and Surface Chemistry*, 3rd ed.; Marcel Dekker: New York, 1997.

(2) Evans, D. F.; Wennerstrom, H. *The Colloidal Domain: Where Physics, Chemistry, Biology, and Technology Meet*; Wiley-VCH: New York, 2001.

(3) Otsubo, Y. Flocculation of Colloids by Soluble Polymers and its Effect on Rheology. *Heterog. Chem. Rev.* **1996**, *3*, 327−349.

(4) Swenson, J.; Smalley, M. V.; Hatharasinghe, H. L. M. Mechanism and Strength of Polymer Bridging Flocculation. *Phys. Rev. Lett.* **1998**, *81*, 5840−5843.

(5) Yu, X.; Somasundaran, P. Role of Polymer Conformation in Interparticle-Bridging Dominated Flocculation. *J. Colloid Interface Sci.* **1996**, *177*, 283−287.

(6) Biggs, S.; Habgood, M.; Jameson, G. J.; Yan, Y. D. Aggregate Structures Formed via a Bridging Flocculation Mechanism. *Chem. Eng. J.* **2000**, *80*, 13−22.

(7) Dickinson, E.; Euston, S. R. Computer-Simulation of Bridging Flocculation. *J. Chem. Soc., Faraday Trans.* **1991**, *87*, 2193−2199.

(8) Stoll, S.; Buffle, J. Computer Simulation of Bridging Flocculation Processes: The Role of Colloid to Polymer Concentration Ratio on Aggregation Kinetics. *J. Colloid Interface Sci.* **1996**, *180*, 548−563.

(9) Dao, V. H.; Cameron, N. R.; Saito, K. Synthesis, Properties and Performance of Organic Polymers Employed in Flocculation Applications. *Polym. Chem.* **2016**, *7*, 11−25.

(10) Hiddessen, A. L.; Rodgers, S. D.; Weitz, D. A.; Hammer, D. A. Assembly of Binary Colloidal Structures via Specific Biological Adhesion. *Langmuir* **2000**, *16*, 9744−9753.

(11) Milam, V. T.; Hiddessen, A. L.; Crocker, J. C.; Graves, D. J.; Hammer, D. A. DNA-Driven Assembly of Bidisperse, Micron-Sized Colloids. *Langmuir* **2003**, *19*, 10317−10323.

(12) Rogers, P. H.; Michel, E.; Bauer, C. A.; Vanderet, S.; Hansen, D.; Roberts, B. K.; Calvez, A.; Crews, J. B.; Lau, K. O.; Wood, A.; Pine, D. J.; Schwartz, P. V. Selective, Controllable, and Reversible Aggregation of Polystyrene Latex Microspheres via DNA Hybridization. *Langmuir* **2005**, *21*, 5562−5569.

(13) Wee, E. J. H.; Lau, H. Y.; Botella, J. R.; Trau, M. Re-Purposing Bridging Flocculation for On-Site, Rapid, Qualitative DNA Detection in Resource-Poor Settings. *Chem. Commun.* **2015**, *51*, 5828−5831.

(14) Wee, E. J. H.; Ngo, T. H.; Trau, M. A Simple Bridging Flocculation Assay for Rapid, Sensitive and Stringent Detection of Gene Specific DNA Methylation. *Clin. Epigenet.* **2015**, *5*, 15028.

(15) Lee, J. H.; Gustin, J. P.; Chen, T. H.; Payne, G. F.; Raghavan, S. R. Vesicle-Biopolymer Gels: Networks of Surfactant Vesicles Connected by Associating Biopolymers. *Langmuir* **2005**, *21*, 26−33.

(16) Dowling, M. B.; Kumar, R.; Keibler, M. A.; Hess, J. R.; Bochicchio, G. V.; Raghavan, S. R. A Self-Assembling Hydrophobically Modified Chitosan Capable of Reversible Hemostatic Action. *Biomaterials* **2011**, *32*, 3351−3357.

(17) Chen, Y. J.; Javvaji, V.; MacIntire, I. C.; Raghavan, S. R. Gelation of Vesicles and Nanoparticles using Water-Soluble Hydrophobically Modified Chitosan. *Langmuir* **2013**, *29*, 15302−15308.

(18) Javvaji, V.; Dowling, M. B.; Oh, H.; White, I. M.; Raghavan, S. R. Reversible Gelation of Cells Using Self-Assembling Hydrophobically-Modified Biopolymers: Towards Self-Assembly of Tissue. *Biomater. Sci.* **2014**, *2*, 1016−1023.

DOI: 10.1021/acsami.7b05435
ACS Appl. Mater. Interfaces 2017, 9, 37238−37245

(19) Tonelli, A. E. Nanostructuring and Functionalizing Polymers with Cyclodextrins. *Polymer* **2008**, *49*, 1725−1736.
(20) Kumar, R.; Raghavan, S. R. Thermothickening in Solutions of Telechelic Associating Polymers and Cyclodextrins. *Langmuir* **2010**, *26*, 56−62.
(21) Arya, C.; Kralj, J. G.; Jiang, K. Q.; Munson, M. S.; Forbes, T. P.; DeVoe, D. L.; Raghavan, S. R.; Forry, S. P. Capturing Rare Cells From Blood Using a Packed Bed of Custom-Synthesized Chitosan Microparticles. *J. Mater. Chem. B* **2013**, *1*, 4313−4319.
(22) Owen, C. A. *A History of Blood Coagulation*; Mayo Foundation: Rochester, MN, 2001.
(23) Smith, G. F. Fibrinogen-Fibrin Conversion - Mechanism of Fibrin-Polymer Formation in Solution. *Biochem. J.* **1980**, *185*, 1−11.
(24) Topol, E. J.; Yadav, J. S. Recognition of the Importance of Embolization in Atherosclerotic Vascular Disease. *Circulation* **2000**, *101*, 570−580.
(25) Rammohan, A.; Sathyanesan, J.; Ramaswami, S.; Lakshmanan, A.; Senthil-Kumar, P.; Srinivasan, U. P.; Ramasamy, R.; Ravichandran, P. Embolization of Liver Tumors: Past, Present and Future. *World J. Radiol.* **2012**, *4*, 405−412.
(26) Loffroy, R.; Pottecher, P.; Cherblanc, V.; Favelier, S.; Estivalet, L.; Koutlidis, N.; Moulin, M.; Cercueil, J. P.; Cormier, L.; Krause, D. Current Role of Transcatheter Arterial Embolization for Bladder and Prostate Hemorrhage. *Diagn. Interv. Imaging* **2014**, *95*, 1027−1034.
(27) Ortega-Vinuesa, J. L.; Bastos-Gonzalez, D. A Review of Factors Affecting the Performances of Latex Agglutination Tests. *J. Biomater. Sci., Polym. Ed.* **2001**, *12*, 379−408.
(28) Desbrieres, J.; Martinez, C.; Rinaudo, M. Hydrophobic Derivatives of Chitosan: Characterization and Rheological Behaviour. *Int. J. Biol. Macromol.* **1996**, *19*, 21−28.
(29) Wu, L. Q.; Yi, H. M.; Li, S.; Rubloff, G. W.; Bentley, W. E.; Ghodssi, R.; Payne, G. F. Spatially Selective Deposition of a Reactive Polysaccharide Layer onto a Patterned Template. *Langmuir* **2003**, *19*, 519−524.
(30) Wei, W.; Wang, L. Y.; Yuan, L.; Wei, Q.; Yang, X. D.; Su, Z. G.; Ma, G. H. Preparation and Application of Novel Microspheres Possessing Autofluorescent Properties. *Adv. Funct. Mater.* **2007**, *17*, 3153−3158.
(31) Zhu, C.; Lee, J. H.; Raghavan, S. R.; Payne, G. F. Bioinspired Vesicle Restraint and Mobilization using a Biopolymer Scaffold. *Langmuir* **2006**, *22*, 2951−2955.
(32) Dowling, M. B.; Bagal, A. S.; Raghavan, S. R. Self-Destructing "Mothership" Capsules for Timed Release of Encapsulated Contents. *Langmuir* **2013**, *29*, 7993−7998.

DOI: 10.1021/acsami.7b05435
ACS Appl. Mater. Interfaces 2017, 9, 37238−37245

Supporting Information for:

Clustering of Cyclodextrin-Functionalized Microbeads by an Amphiphilic Biopolymer: Real-Time Observation of Structures Resembling Blood Clots

Chandamany Arya, Camila A. Saez Cabesas, Hubert Huang and Srinivasa R. Raghavan*
Department of Chemical and Biomolecular Engineering, University of Maryland, College Park, MD 20742-2111
*Corresponding author. Email: sraghava@umd.edu

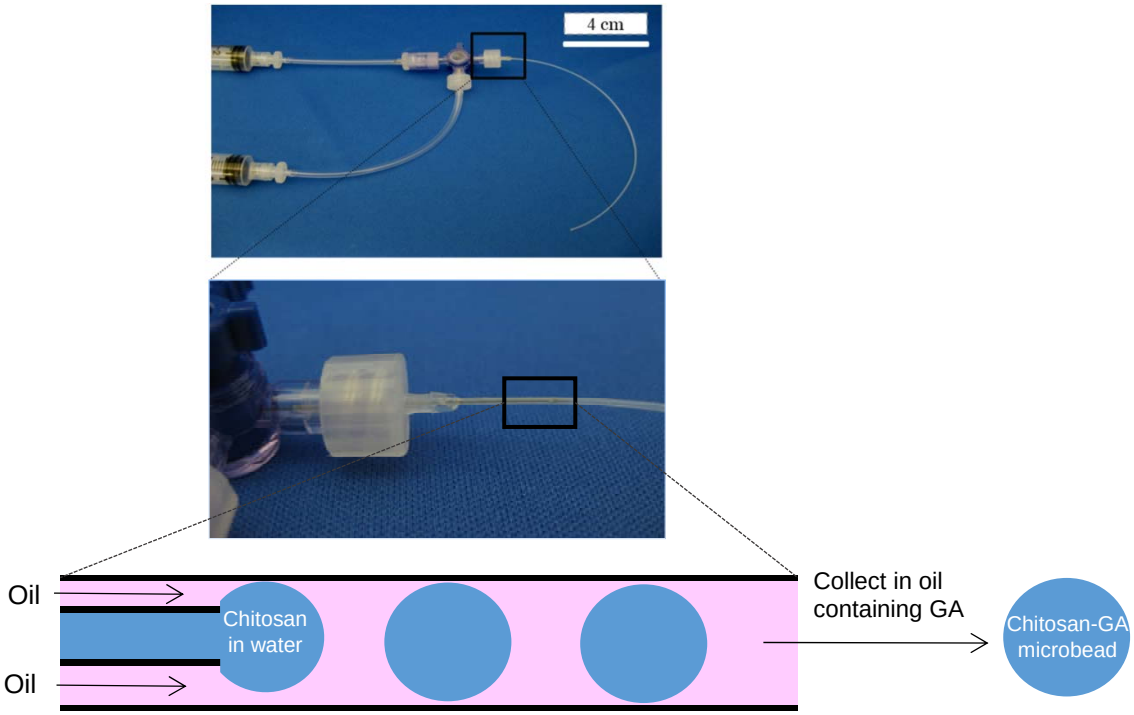

Figure S1. Co-flow microfluidic tubing device used to prepare chitosan-GA microbeads. Photographs of the device are shown on the top and a schematic of the droplet formation process is shown on the bottom. An aqueous solution of 2 wt% chitosan in 0.2 M acetic acid is fed through the inner silica capillary at 1.5 µL/min. An oil phase (hexadecane with 2 wt% Span 80) is flowed through the outer Teflon tube at 30 µL/min. In the process, uniform aqueous droplets with a diameter ~ 160 µm are formed, and these are collected in a cross-linking solution of 2 wt% GA in hexadecane (with 2 wt% added Span 80). The droplets are allowed to cross-link for 20 h to form the chitosan-GA microbeads.

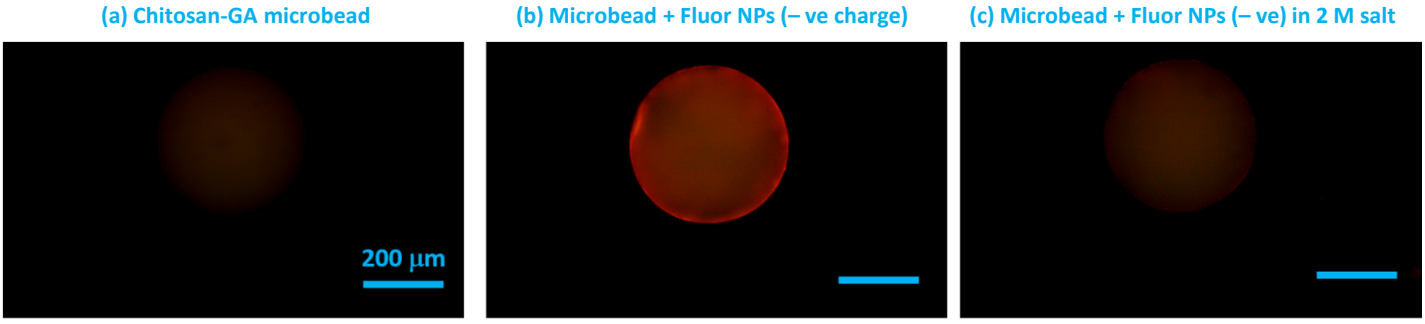

Figure S2. Evidence for the residual positive charge on chitosan-GA microbeads. (a) Initial beads show weak autofluorescence at all wavelengths. (b) When the beads are combined with negatively charged red-fluorescent nanoparticles (NPs) in water, the NPs adsorb due to electrostic interactions onto the bead surface. After washing, the fluorescence intensity is 2.5× the initial value in (a). (c) When the beads are combined with the NPs in 2 M NaCl, the adsorption is weaker, due to the screening of electrostatic interactions by the salt ions. In this case, the fluorescence intensity is only 1.3× that in (a). All scale bars are 200 µm.

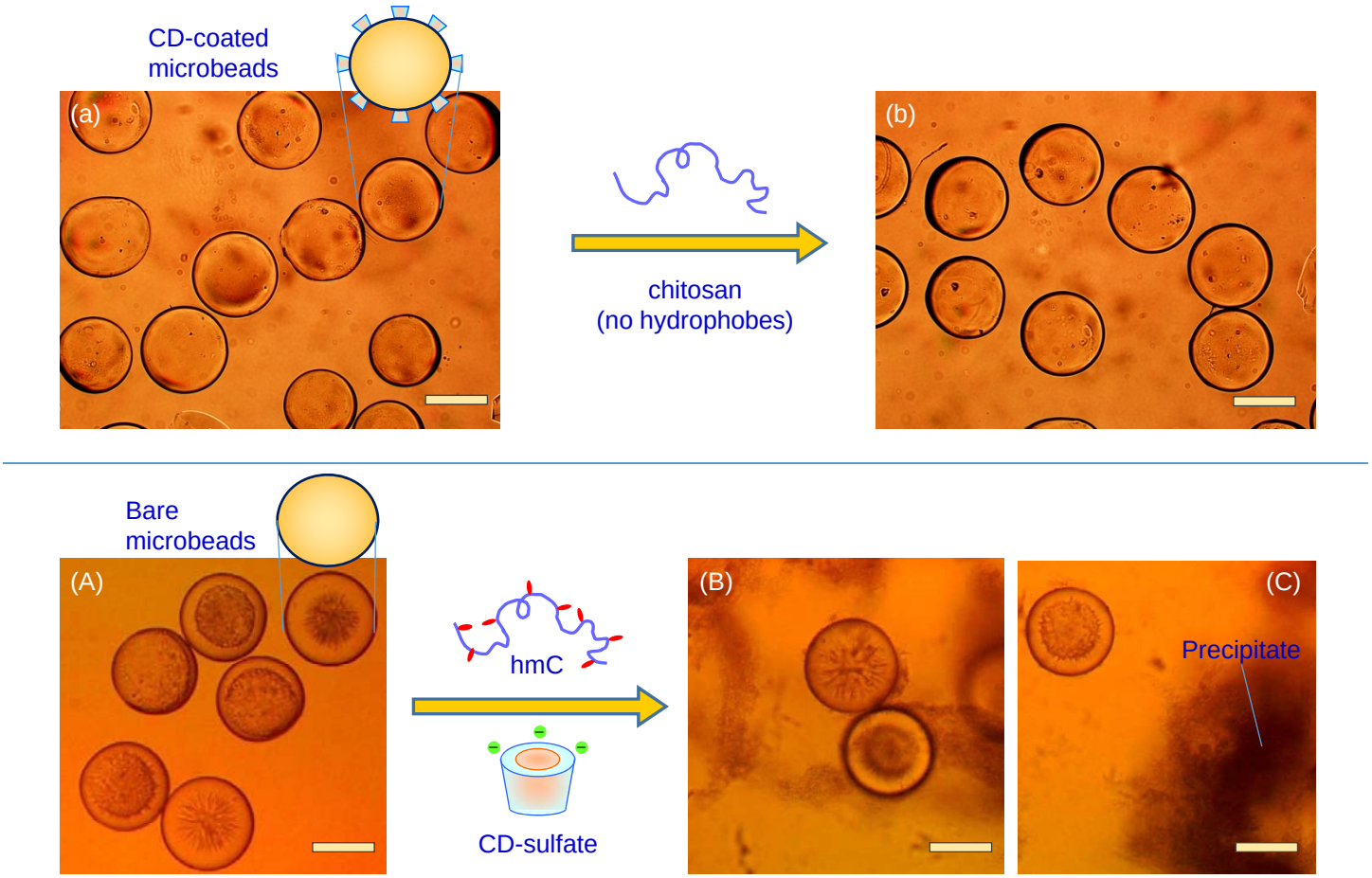

Figure S3. Evidence that microbead clustering requires both CD-coated beads as well as hmC. (Top Panel) When CD-coated beads (a) are combined with native chitosan (lacking hydrophobes), no clustering is observed (b). (Bottom Panel) When bare beads (with no CD on their surfaces) (A) are combined with both hmC as well as CD-sulfate, a precipitate forms in the solution around the beads (B and C), but there is negligible clustering of the beads, nor is there a polymer mesh around them. All scale bars are 100 µm.

Stage 1: Microbeads form clusters due to the action of hmC

Analogous Stage 1: Platelets from blood aggregate at the wound site

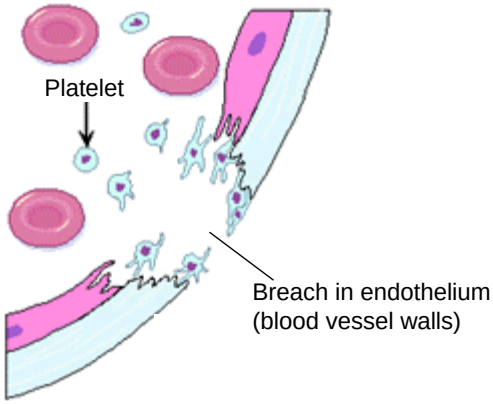

Stage 2: hmC from solution precipitates on the microbeads to form a mesh around the clusters

Analogous Stage 2: Fibrinogen activated by thrombin to form fibrin mesh around the platelets

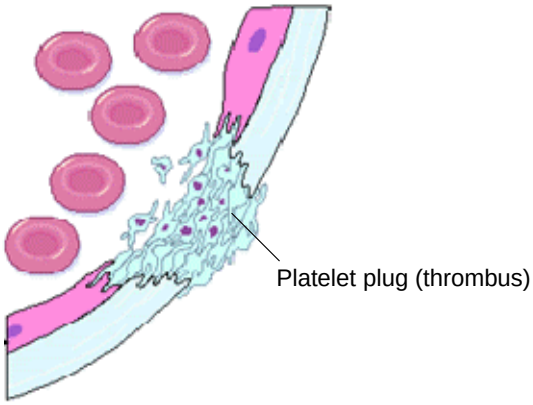

Consequence: hmC mesh entraps and immobilizes inert beads in the cluster

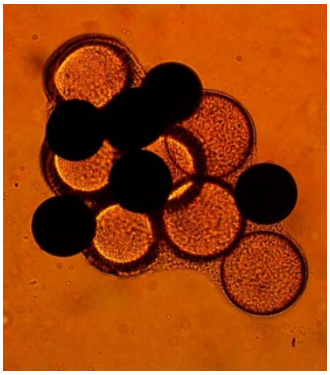

Analogous Consequence: Fibrin mesh entraps inert blood cells and thereby forms a plug (clot).

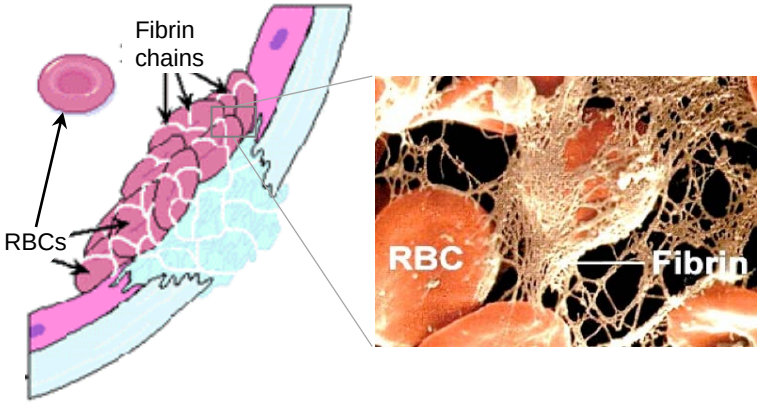

Figure S4. Analogy between the clustering of CD-coated beads by hmC and blood clotting. Both processes occur in two distinct stages, as indicated by the schematics. In the latter process, the platelets initially aggregate into a plug, and then a mesh of fibrin is induced around this plug. The fibrin mesh entraps inert blood cells.

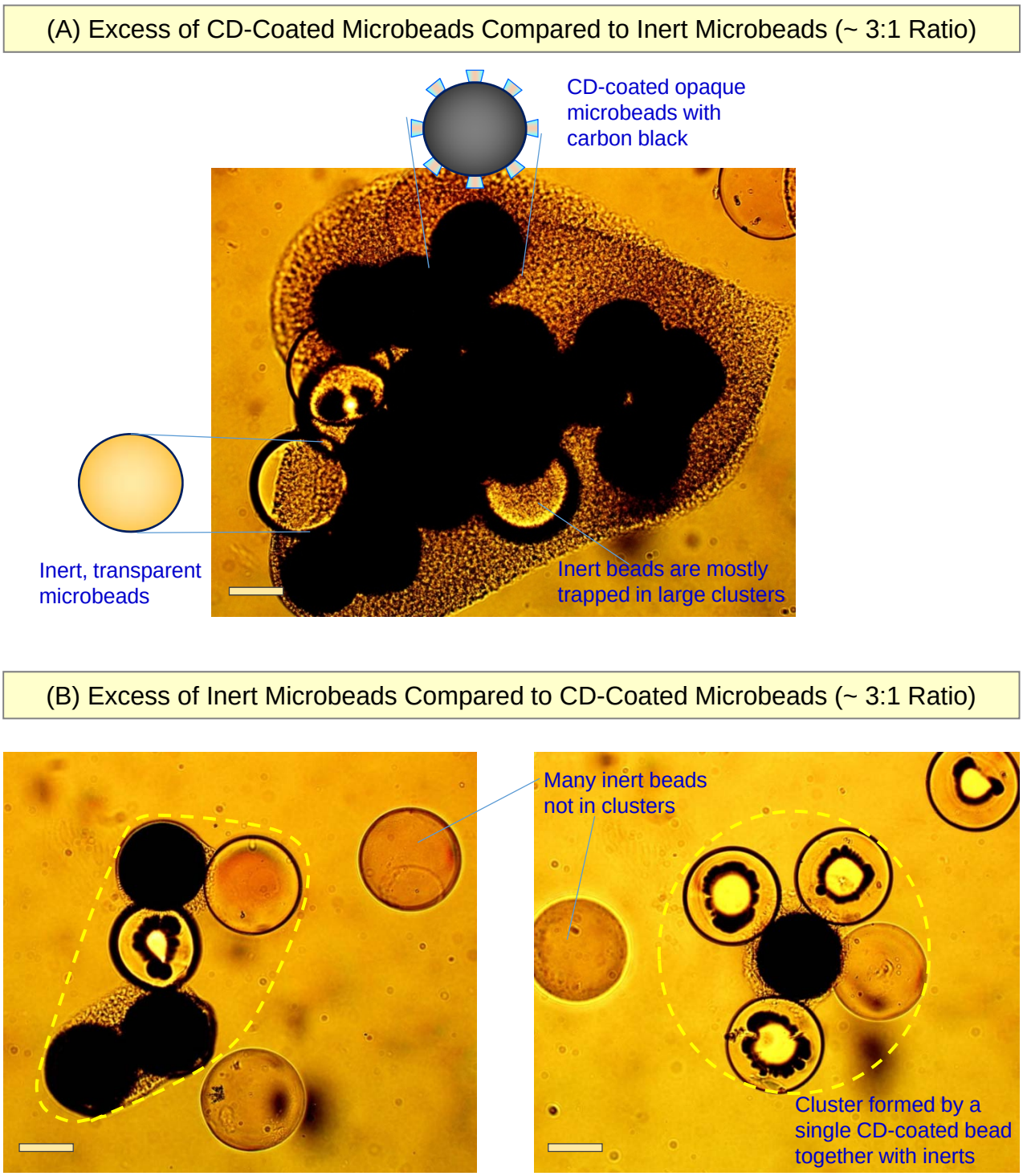

Figure S5. Different cluster morphologies when the ratio of CD-coated beads to inert beads is altered. Here, the CD-coated beads are opaque due to encapsulated carbon black while the inert ones are transparent. Both have diameters ~ 150 µm. Clustering is induced by adding 0.25 wt% hmC. (A) The ratio of CD-coated to inert beads is maintained around 3:1, i.e., there is an excess of the former. In this case, large clusters are seen, and most of the inerts are trapped in such clusters. Note that an hmC mesh surrounds the entire cluster. (B) The ratio of CD-coated to inert beads is 1:3, i.e., there is an excess of the latter. In this case, the clusters are smaller and contain fewer particles. Some clusters have only a single CD-coated bead, but the hmC mesh around this bead still causes it to bind to several inerts. Also, several inert beads are observed to be discrete and not part of any clusters. Scale bars in all the images are 100 µm.